Nonlinear, interacting responses to climate limit grassland production under global change

Kai Zhu[a,b,c,1], Nona R. Chiariello[d], Todd Tobeck[a], Tadashi Fukami[b], and Christopher B. Field[a]

[a]Department of Global Ecology, Carnegie Institution for Science, Stanford, CA 94305; [b]Department of Biology, Stanford University, Stanford, CA 94305; [c]Department of BioSciences, Rice University, Houston, TX 77005; and [d]Jasper Ridge Biological Preserve, Stanford University, Stanford, CA 94305

Edited by William H. Schlesinger, Cary Institute of Ecosystem Studies, Millbrook, NY, and approved July 22, 2016 (received for review April 28, 2016)

Global changes in climate, atmospheric composition, and pollutants are altering ecosystems and the goods and services they provide. Among approaches for predicting ecosystem responses, long-term observations and manipulative experiments can be powerful approaches for resolving single-factor and interactive effects of global changes on key metrics such as net primary production (NPP). Here we combine both approaches, developing multidimensional response surfaces for NPP based on the longest-running, best-replicated, most-multifactor global-change experiment at the ecosystem scale—a 17-y study of California grassland exposed to full-factorial warming, added precipitation, elevated CO_2, and nitrogen deposition. Single-factor and interactive effects were not time-dependent, enabling us to analyze each year as a separate realization of the experiment and extract NPP as a continuous function of global-change factors. We found a ridge-shaped response surface in which NPP is humped (unimodal) in response to temperature and precipitation when CO_2 and nitrogen are ambient, with peak NPP rising under elevated CO_2 or nitrogen but also shifting to lower temperatures. Our results suggest that future climate change will push this ecosystem away from conditions that maximize NPP, but with large year-to-year variability.

California grassland | climate change | ecosystem ecology | global change experiment | Jasper Ridge

Across the globe, terrestrial ecosystems are experiencing simultaneous changes in climate, atmospheric composition, pollutant deposition, and broad-scale changes in land use, biological invasions, and disturbance regimes, including wildfire. How ecosystems respond will have profound consequences for the goods and services they provide for humans, including feedbacks to atmospheric composition and climate. Predicting ecosystem responses to these global changes is challenging due to the number of factors and the possibility of interactive effects across physiological, ecological, and biogeochemical aspects of ecosystem function. Manipulative experiments, which can resolve single-factor and interactive effects, can effectively address these challenges, especially when focused on metrics such as net primary production (NPP) that integrate across many levels of response. For example, experiments combining warming and elevated atmospheric CO_2 have mostly reported increases in NPP, with stimulatory effects of elevated CO_2 partially eroded by the effects of warming (1). Experiments combining either of these factors with other treatments have been diverse, with the magnitude of ecosystem responses generally decreasing as the number of global-change factors increases (2, 3). However, four difficulties complicate the interpretation of multifactor global-change experiments: Few experiments incorporate a realistic range of interacting factors, making it difficult to connect experimental with real-world responses; most experiments involve only two levels of each factor (e.g., ambient and +2 °C warming), making it difficult to characterize response surfaces; most experiments entail too few replicates to identify subtle effects; and few experiments continue long enough to determine time dependence in responses.

Here we use 17 y of data from the Jasper Ridge Global Change Experiment (JRGCE) to test for single-factor, interactive, nonlinear, and progressive effects of four global change factors—warming, added precipitation, elevated CO_2, and nitrogen deposition—on grassland NPP and its components aboveground NPP (ANPP) and belowground NPP (BNPP). Located in central coastal California, the JRGCE has a Mediterranean climate with cool, wet winters and warm, dry summers, defining a roughly 7-mo growing season, typically November to May. The vegetation is a mix of naturalized and native grasses and forbs. Over the course of the experiment, harvested aboveground biomass was 71.3% annual and 28.7% perennial (Fig. S1). Of 54 annual plant taxa in the JRGCE, 81% are nonnative to California, including all of the annual grasses; of 20 perennial taxa, 55% are native, including all perennial grass species except one. All of the plant species have the C3 photosynthesis pathway. The experiment includes two levels of four treatment factors—ambient conditions and elevated warming (+80–+250 $W \cdot m^{-2}$), precipitation (+50%), CO_2 (+275 $\mu mol \cdot mol^{-1}$), and nitrogen deposition (+7 $g \cdot m^{-2} \cdot y^{-1}$)—with eight replicates (blocks) of all 16 possible combinations (128 plots, plus another eight infrastructure-free controls) (*Methods*). The JRGCE framework has provided access to global change effects on nutrient interactions (4), phenology (5, 6), plant and microbial community composition (7, 8), trophic relationships (9), and many other aspects of ecosystem function reported in over 50 publications. Here we analyze primary production from 1998 (a pretreatment year) and 16 y of treatments.

Across treatments and years, NPP varied by a factor of three (518–1,647 $g \cdot m^{-2} \cdot y^{-1}$), commensurate with variation in ANPP (218–1,142 $g \cdot m^{-2} \cdot y^{-1}$) and BNPP (173–784 $g \cdot m^{-2} \cdot y^{-1}$). Using several approaches, we tested for but found no consistent year-to-year temporal trends in the sign, magnitude, or significance of single-factor or interactive effects of the global change factors on NPP or its components (*Methods* and *SI Text*). In addition, there

Significance

Global environmental change involves many factors that occur simultaneously, yet they are usually studied in isolation. Here we report a long-term global change experiment that subjected California grassland to multiple individual and simultaneous changes in temperature, precipitation, carbon dioxide, and nitrogen. Our analysis revealed nonlinear and interactive effects of temperature and precipitation on grassland net primary production (NPP), which defined a ridge-shaped NPP response surface to these two variables. Added nitrogen raised the peak of the NPP response surface, and added CO_2 shifted the peak to lower temperatures. Our approach was validated by tests showing an absence of progressive effects over the years. In other ecosystems, our approach may be similarly powerful for probing the effects of multifactor global change.

Author contributions: N.R.C. and C.B.F. designed research; K.Z., N.R.C., T.T., and C.B.F. performed research; K.Z. analyzed data; and K.Z., N.R.C., T.F., and C.B.F. wrote the paper.

The authors declare no conflict of interest.

This article is a PNAS Direct Submission.

Freely available online through the PNAS open access option.

[1]To whom correspondence should be addressed. Email: kai.zhu@rice.edu.

This article contains supporting information online at www.pnas.org/lookup/suppl/doi:10.1073/pnas.1606734113/-/DCSupplemental.

were no consistent year-to-year trends in the relative abundance of the major plant functional groups (Fig. S1). The absence of time dependence opens a novel path for analyzing primary production—treating years as independent realizations of the experiment, and analyzing NPP, ANPP, and BNPP as continuous functions of each of the four global change factors. This approach takes advantage of 17 y of natural variation in temperature and precipitation as well as the treatments, which together filled the environmental space nearly uniformly across a 3.6 °C range in mean temperature during the growing season and a sixfold variation in precipitation (240–1,379 mm). CO_2 and nitrogen levels remain nearly categorical owing to background variation and trends that are small relative to the magnitude of the treatments (Fig. 1). This approach allows consideration of many sources of variation, including fires in 2003 and 2011 that are not discussed here (*Methods*). Although the analytical model tests simultaneously for single-factor and interaction effects, we start by discussing the single-factor responses of NPP, ANPP, and BNPP. Then, we explore combined single-factor and interactive effects of the continuous factors and test for progressive

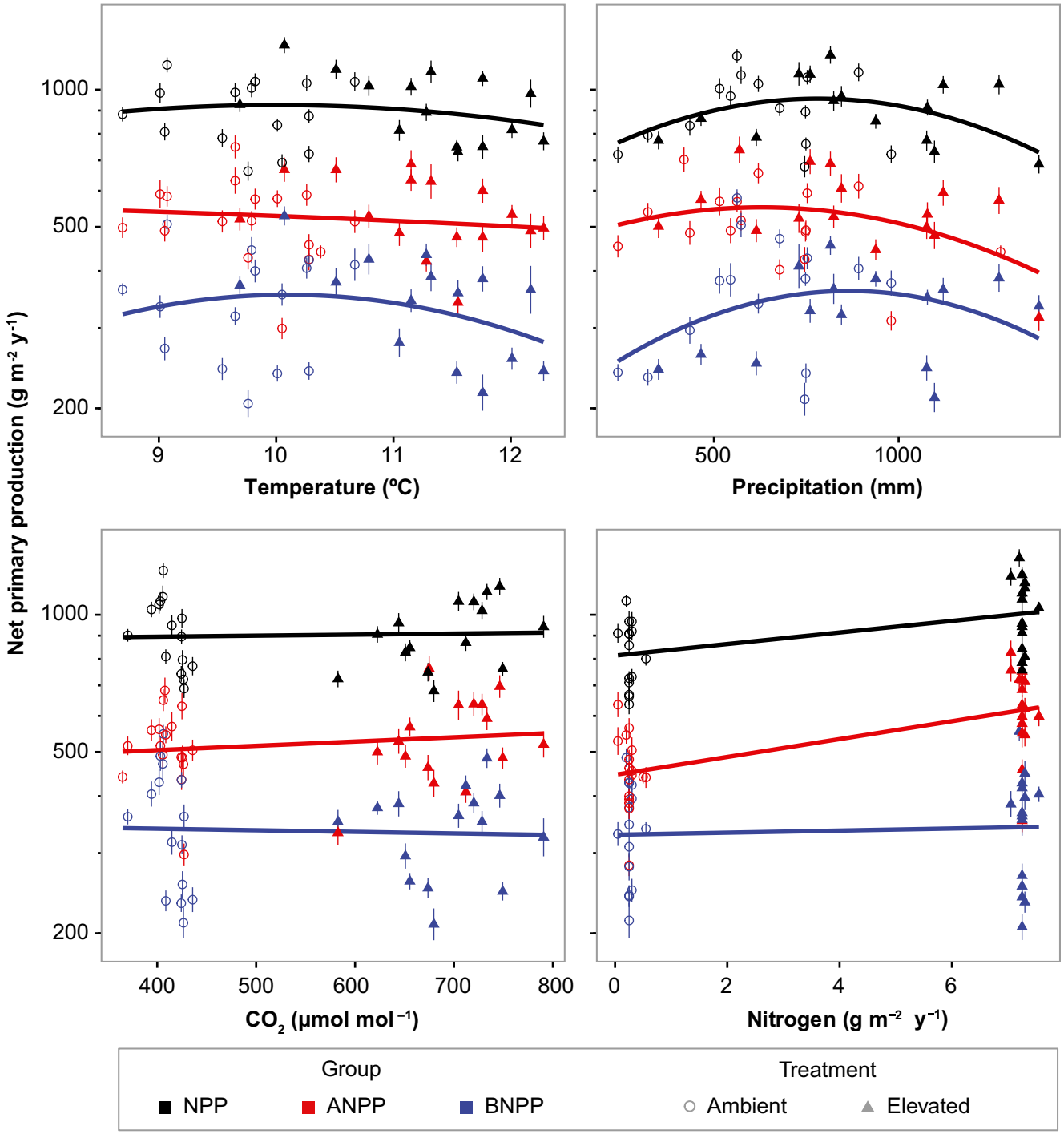

Fig. 1. Responses of NPP and its components ANPP and BNPP to temperature, precipitation, CO_2, and nitrogen across experimental (treatment) and natural (year) variation. Each symbol represents the average production (mean ± SE) in the ambient (open circle) or elevated (filled triangle) treatment in 1 y.

effects. Finally, we use the results of the continuous model to create temperature-by-precipitation response surfaces for NPP under the four factorial combinations of CO_2 and nitrogen.

Single-factor responses vary in form and magnitude across the global change factors (Fig. 1). Warming generally had negative effects on production, with a slightly hump-shaped (unimodal) response for BNPP. Responses to precipitation are hump-shaped, peaking when precipitation is near (ANPP) or slightly above (BNPP and NPP) the 40-y mean growing season precipitation at Jasper Ridge (590 mm). Elevated CO_2 had no significant impact, tending to increase ANPP and decrease BNPP, summing to no response for NPP. Nitrogen addition increased ANPP by 38%, BNPP by 4%, and NPP by 23% (Fig. 1).

We developed linear mixed-effects models (*Methods* and *SI Text*) that provide results for both the main and interactive effects as standardized coefficients (Fig. 2 and Table S1). These coefficients indicate the proportional change in NPP in response to one SD change in an environmental factor. The model fit to observations is good, with 54–68% agreement, and the residuals do not show time dependence, providing additional evidence of a lack of progressive effects (*Methods* and *SI Text*). The main effects from the joint model reinforce the patterns in the single-factor plots (Figs. 1 and 2). The quadratic coefficients for temperature and precipitation are negative for production components that have hump-shaped responses to those factors, and the temperature and precipitation coefficients are negative for production terms that decline linearly or peak at low values. BNPP, the only term that peaks at higher levels of precipitation, has a positive precipitation coefficient. Main effects of nitrogen are positive and substantial for NPP and ANPP, corresponding to more than a 20% increase in both ANPP and NPP at the elevated treatment level. Elevated CO_2 has no consistent effect on NPP (Fig. 2). In addition to the main effects, five interactions are significant. The temperature–precipitation interaction is positive for NPP, indicating that the negative effects of warming and precipitation are intensified when combined. Other two-way interactions involve factors whose main effects are opposite in sign; their interpretation is aided by the response surfaces that follow.

The modeled main effects and interactions define multidimensional response surfaces in which the response of NPP to temperature and precipitation is basically a ridge, with maximum NPP occurring at intermediate levels of precipitation and

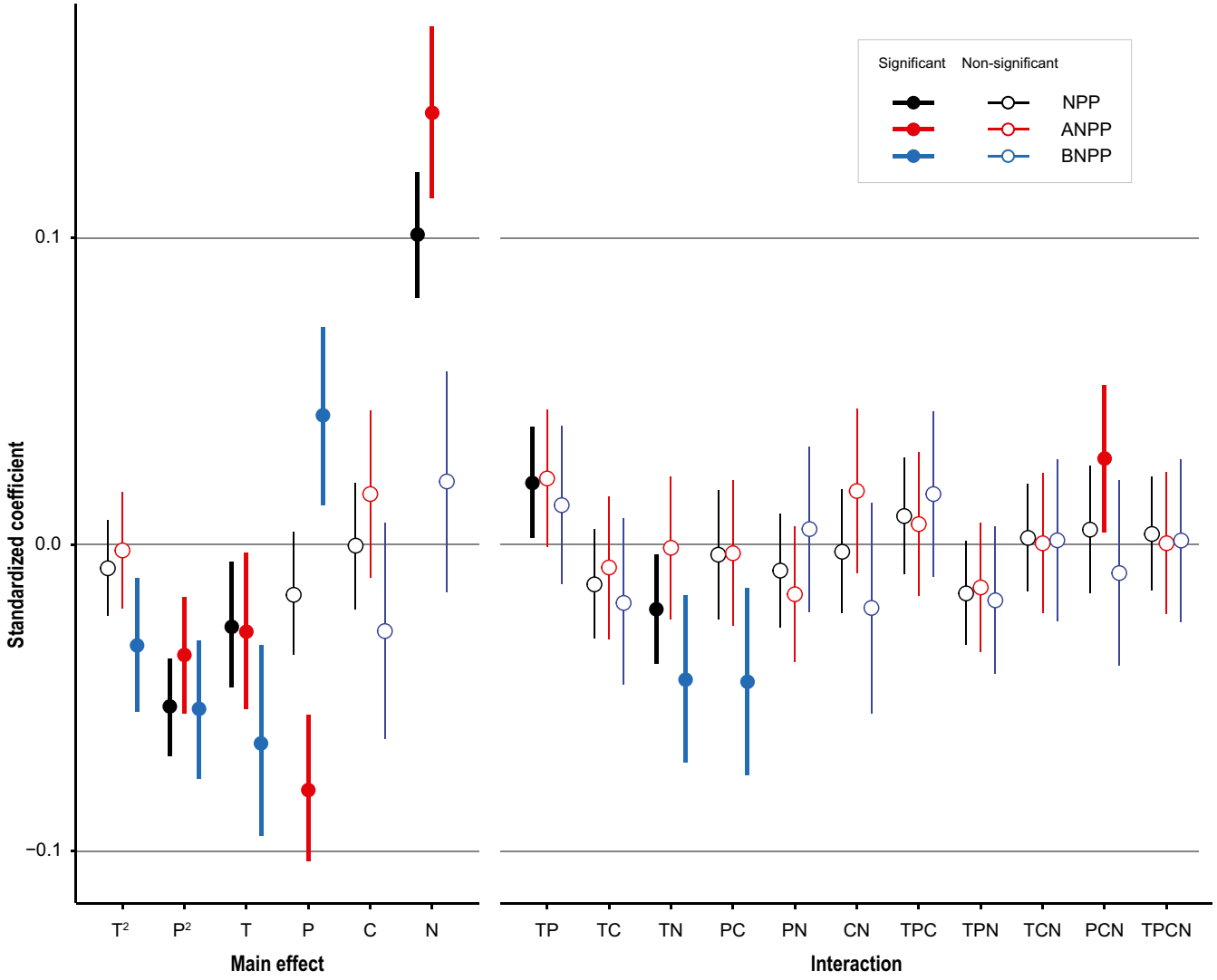

Fig. 2. Main effects and interactions of temperature (T), precipitation (P), CO_2 (C), and nitrogen (N), and quadratic effects of temperature (T^2) and precipitation (P^2), on primary production. Coefficients are summarized as point estimates (circles) and 95% confidence intervals (CIs, lines) for NPP and its components (colors), highlighting significant coefficients (filled circles) whose 95% CIs do not overlap zero (bold lines). Coefficients are standardized as proportional change in primary production with respect to one SD change in T, P, C, and N (T: 0.99 °C, P: 289 mm, C: 148 μmol·mol^{-1}, and N: 3.55 g·m^{-2}·y^{-1}).

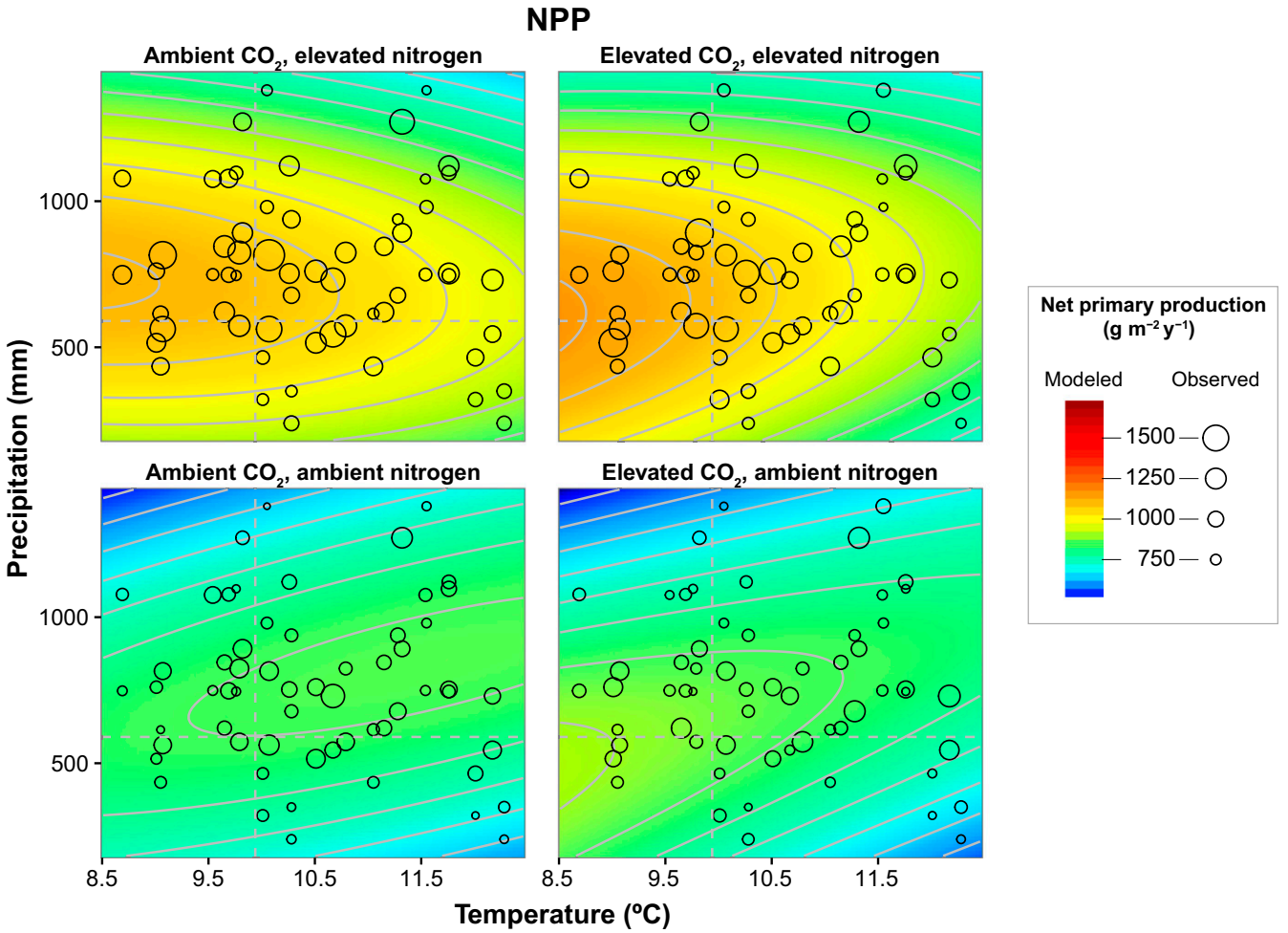

Fig. 3. Modeled and observed NPP in four-dimensional temperature–precipitation–CO_2–nitrogen space. Axes are continuous gradients for temperature (8.69–12.28 °C) and precipitation (240–1,380 mm), as well as categorical levels for CO_2 (ambient 409 μmol·mol^{-1}, elevated 680 μmol·mol^{-1}) and nitrogen (ambient 0.25 g·m^{-2}·y^{-1}, elevated 7.25 g·m^{-2}·y^{-1}). Observed values (bubbles) are the average NPP in the corresponding environmental conditions. Modeled values (surfaces with contour lines) are predictions from models fitted with observations spanning the environmental space. Dashed lines are references of long-term averages of temperature and precipitation at Jasper Ridge.

temperature (Fig. 3). When CO_2 or nitrogen deposition is elevated, the peak of the NPP ridge is higher and displaced to cooler temperatures, sloping downward as temperature increases. The precipitation that maximizes NPP drops from about 800 mm at ambient CO_2 to about 600 mm at elevated CO_2 (Fig. 3). The response surfaces are similar for the above- and belowground components of NPP (Figs. S3 and S4), but with ANPP reaching its maximum under drier conditions, and BNPP under wetter conditions.

The responses of NPP to nitrogen deposition parallel results from other studies. Like grasslands globally (10–12), California annual grassland is nitrogen-limited, and nitrogen deposition relieves some of this limitation (13–15). The absence of single-factor effects of elevated CO_2—with trends toward a small positive effect on ANPP and a slight negative effect on BNPP—are consistent with earlier results from Jasper Ridge (14–16) and confirm earlier results indicating lower CO_2 sensitivity than reported for other grasslands (12, 17). The shift of maximum NPP to drier conditions under elevated CO_2 (Fig. 3) is consistent with improved water-use efficiency in plants with C3 photosynthesis growing under elevated CO_2 (18).

The response of NPP to temperature points to effects of multiple controls on photosynthesis and growth. Under ambient nitrogen deposition, the effects of warming on NPP depend on precipitation—NPP declines with rising temperature at low precipitation but increases with temperature at high precipitation. With elevated nitrogen deposition, warming leads to decreased NPP at all precipitation levels. Under ambient nitrogen, the optimum temperature for NPP is close to the long-term average, 9.94 °C, but it drops to about 1 °C lower with nitrogen deposition (dashed lines in Fig. 3). The negative effect of warming likely is influenced by NPP gains in winter outweighed by losses in spring. Gains in NPP from warmer winter temperatures are small because plant growth in winter is also limited by low irradiance and short days (16). In spring, when conditions are consistent with rapid biomass accumulation by vegetative plants, warming decreases NPP through accelerated phenology: Warming hastens flowering (6) and senescence (5) in the JRGCE, effectively wasting part of the growing season.

Elevated CO_2 has subtle effects on the response surface (compare left and right panels in Fig. 3), shifting peak NPP to lower temperatures. Because this is opposite the response expected based on the physiology of C3 photosynthesis (19), it may reflect a temperature sensitivity of autotrophic respiration or exudation larger than that of photosynthesis.

The hump-shaped response of NPP to precipitation helps unify divergent results about the dependence of California grassland NPP on the amount and timing of precipitation (20–22). Had our experiment spanned significantly less than a sixfold range in precipitation, we would have concluded that NPP increased,

decreased, or was unaffected by variation in annual precipitation. Had our precipitation treatment significantly altered the seasonal distribution of rainfall, rather than amplifying natural variation, shifts in plant community composition likely would have altered the NPP response (22).

Nonlinear responses of ANPP to precipitation occur in other grasslands and other biomes (23–25) but tend to be saturating rather than the symmetrical NPP response we observe. Decreasing NPP at very high precipitation input at Jasper Ridge may be related to generally cloudy growing seasons in the wettest years or to nutrient leaching, especially with the highest (manipulated) inputs. Evidence that extremely high rainfall can be detrimental to grassland NPP is supported by measurements of ecosystem carbon balance. The wettest year during the JRGCE treatments (2006 growing season) had the lowest ANPP, and, based on CO_2 balance, the grassland was a net carbon source (16). The next year was dry, ANPP doubled, and the ecosystem was a net carbon sink (16).

At Jasper Ridge and in grasslands globally, year-to-year variation in temperature and precipitation is substantial, often dramatic. In the JRGCE, the combination of single-factor and interactive effects results in NPP peaking under conditions close to the historic averages and falling off when a year is, as a result of either natural variability or experimental manipulation, substantially different from the average. If this kind of response is typical across grasslands and other ecosystems adapted to interannual variability, future climate change will tend to erode NPP as conditions diverge from historic. Changes in disturbance, herbivory, pests, pathogens, or other agents that alter plant community composition and function potentially can, of course, lead to additional layers of responses.

Many papers have discussed the expected role of progressive effects (26), but their absence in the NPP responses of the JRGCE is not entirely surprising. First, the large interannual variation in climate may act as an effective reset mechanism. Second, the species mix is largely reset annually, based on natural seed rain from within the plots as well as the surrounding vegetation. These tendencies toward an annual reset are reinforced by the predominance of nonnative, weedy species. Third, the absence of strong responses to elevated CO_2 means that carbon inputs to the soil are not changing consistently over time, limiting one potentially directional driver. Although progressive effects can be important in some ecosystems (e.g., ref. 27), they are only part of the diverse palette of ecosystem responses to a changing climate.

Methods

Experiment. The JRGCE is located in the Jasper Ridge Biological Preserve, San Mateo, California (37°24′N, 122°14.5′W). The site occupies ∼0.75 ha within a 5-ha stand of California annual and perennial grassland and has a Mediterranean climate with cool, wet winters and warm, dry summers. Over the period from 1998 to 2014, annual precipitation, which occurs almost entirely from November through April, varied from 240 to 1,280 mm. In summer 1997, we established 36 circular plots 2 m in diameter, subdivided into four equal-sized subplots. The 1997–1998 growing season (year 1) was a pretreatment year, after which treatments were applied for 16 consecutive growing seasons (years 2–17), from the time of germination (November) to plant senescence (June).

Treatments consisted of four global change factors—temperature, precipitation, CO_2, and nitrogen—at either ambient or an elevated level, applied in a complete factorial, randomized block design with eight replicates. Factorial combinations of CO_2 (via free-air CO_2 enrichment) and warming (via heaters suspended above the plot) were applied at the whole-plot level. The CO_2 treatment was targeted at +300 $\mu mol \cdot mol^{-1}$ over background via free-air CO_2 enrichment; the actual enrichment was +275.3 $\mu mol \cdot mol^{-1}$ over the level measured in low plots, which averaged +32.8 $\mu mol \cdot mol^{-1}$ higher than the CO_2 concentration measured at the Mauna Loa observatory (28). The warming treatment increased from +80 $W \cdot m^{-2}$ (years 2–5), to +100 $W \cdot m^{-2}$ (years 6–12), to +250 $W \cdot m^{-2}$ (years 13–17). Within each plot, the four subplots received factorial combinations of precipitation (via emitters mounted outside the plot perimeter) and nitrogen deposition (via nitrate addition). The precipitation treatment was +50% of ambient rainfall, plus two 10-mm additions after the last rainfall event. The nitrogen treatment was +2 g $N \cdot m^{-2} \cdot y^{-1}$ as nitrate solution in November and +5 g $N \cdot m^{-2} \cdot y^{-1}$ as nitrate pellets in late January or early February. An additional four plots (eight subplots) served as controls for the treatment infrastructure and received no treatments. A wildfire spread into the JRGCE in July 2003, affecting two blocks of the experiment. In July 2011, replicate prescribed burns were carried out across four of the blocks, including the two blocks that burned in 2003.

The ecosystem responses included NPP (grams per square meter per year) and its components ANPP and BNPP, which were measured as dry biomass. For aboveground biomass, we harvested all plant matter in a 141-cm^2 area in each subplot at the peak of standing biomass. In years 1–3 we harvested biomass once (in May), and in years 4–17 we harvested from each subplot twice: the first one timed to peak biomass in the phenologically most advanced plots (mid-April to early May), and the second one 3 wk later at the peak of less advanced plots (early to late May). The locations shifted each year to avoid harvesting the same spot for at least three years. In both harvests, we separated out the litter and weighed the oven-dried biomass (70 °C). In this study, we analyzed the aboveground biomass from the single harvest (years 1–3) and the maximum of the two harvests (years 4–17). After the first aboveground harvest we took four soil cores from the harvested area, two shallow (0–15 cm) and two deeper (15–30 cm), and the cores from a given depth were combined and weighed. Roots were removed by a combination of washing and hand-picking, and then were dried and weighed. This procedure was applied to the entire soil sample from each depth except in 1999, when roots were removed from a weighed subsample of soil. In 1999–2003 and 2011 we used manual slide-hammer corers; in 2004–2007 we used a pneumatic corer that removed multiple cores simultaneously, and in 2008–2010 and 2012–2014 we used a single-core pneumatic corer. To account for possible differences in these corers, we calculated an area-based measure of root biomass from the root biomass in the sample together with the core weight, gravimetric soil moisture, and soil bulk density. These values were highly correlated ($R^2 > 0.9$) with measurements based on root biomass and core diameter. No cores were processed in 1998 or 2007, so there are no BNPP or NPP values for those years. In 1999, 2001, and 2006, no deep cores were taken, and we estimated the deep root biomass as the plot-specific average in other years. Across all plots and years, root biomass at 15–30 cm was about one quarter that of 0–15 cm. To account for root turnover, we multiplied the root biomass by 1.54 to obtain final BNPP values (29).

Analysis. We began by testing time-dependent treatment effects (progressive effects) using standard ANOVAs. Fig. S2 shows the ANOVA coefficients of treatment effects (elevated vs. ambient) on log-transformed (to satisfy normality) primary production (NPP, ANPP, and BNPP). We found that treatment effects are mostly nonsignificant except for nitrogen. These treatment effects do not show trends in the sign, magnitude, or significance over 17 y. Both findings are consistent with Dukes et al. (14). The absence of time dependence leads us to integrate experimental treatment and natural variation over 17 y, by quantifying the actual environment each plot experienced.

We characterized the environment in terms of four continuous variables and two factor variables. For temperature (T), we used data from a Jasper Ridge weather station to calculate the average ambient air temperature during the growing season, defined as the 184-d period from the mean date of germination in fall to the mean midpoint between the two harvest dates; for warmed plots we added the mean effect of the warming treatments (1 °C, 1.5 °C, and 2 °C for the three successive generations of heaters). For precipitation (P), we summed rainfall from the first germinating event until the harvest date to obtain ambient values; for treated plots, we augmented this by the amount of rainfall supplements. Both the ambient and elevated CO_2 concentration (C) was measured hourly, at the level of the plant canopy, using an infrared gas analyzer (IRGA) calibrated against a reference traceable to the National Oceanic and Atmospheric Administration network. As a check on CO_2 concentration in the elevated plots, we used a CO_2 fractionation model (30), assuming c_i/c_a is the same for plants at ambient and elevated CO_2 (31), in combination with the $\delta^{13}C$ values in harvested plant tissue and the $\delta^{13}C$ of the fumigation CO_2. The calculation based on the $\delta^{13}C$ of the plants indicated an average elevated CO_2 of 717 $\mu mol \cdot mol^{-1}$, confirming that the plants experienced approximately the CO_2 concentration that the IRGA measured. For nitrogen (N), we determined ambient nitrogen deposition from annual maps from the National Atmospheric Deposition Program (32). The elevated nitrogen deposition was calculated as the ambient value plus the 7 $g \cdot m^{-2} \cdot y^{-1}$ that we applied manually. For the fire in 2003 (F03), we created a factor variable for the following year (2004) to represent whether or not the plot was burned. Likewise, we created another factor variable for the burn in 2011 (B11) for the plots in the following year (2012). We present pairwise relationships between primary production and global change factors (T, P, C, and N) in Fig. 1.

To understand ecosystem responses to multifactor global changes, we used linear mixed-effects models to analyze NPP, with main and interactive global change factors as fixed effects and plot as random effects (33). For main-effects terms, we used linear functions for T, P, C, N, F03, and B11, as well as quadratic functions for T^2 and P^2. Our choice of quadratic functions was motivated by the pairwise relationships in Fig. 1 and verified by model comparison (next paragraph). For interaction terms, we used full factorial combinations of global change factors (TP, TC, TN, PC, PN, CN, TPC, TPN, TCN, PCN, and TPCN). NPP variables (NPP, ANPP, and BNPP) were log-transformed to satisfy normality, and environmental variables (T, P, C, and N) were standardized (subtracting the mean and dividing by SD). The standardization makes coefficients comparable among global change factors. Because of the log-scale NPPs and standardized environmental variables, the estimated fixed effects (main and interaction terms) should be interpreted as proportional change in production ($d \log y$) with respect to an SD change in environment (dx, where x is a SD of T, P, C, or N): $d\log y/dx = (dy/y)/dx$. Likewise, the fire effects should be interpreted as proportional change in production with respect to whether or not the plot-subplot had burned in the wildfire (F03) or prescribed burn (B11). We summarized the estimated coefficients of global change factors (T, P, C, and N) in Fig. 2 and the estimated coefficients of global change factors (T, P, C, and N) and fires (F03 and B11) in Table S1. Our analysis controls for fire effects but focuses on environmental effects.

To verify the model's nonlinear terms, we used an information-theoretic approach for model comparison. We separately fitted (*i*) linear model, with predictors of linear and interaction terms of global change factors, and (*ii*) nonlinear model, with the same linear predictors as in *i* plus quadratic temperature (T^2) and precipitation (P^2) terms. We calculated their Akaike information criterion (AIC) values respectively. AIC measures the relative quality of models for a given set of data, by estimating the information lost when the model represents the process that generates the data. Practically, AIC rewards goodness of fit (likelihood) and penalizes overfitting (number of parameters). A lower AIC indicates a preferred model. Table S2 shows the AIC values of linear and nonlinear models for NPP, ANPP, and BNPP. In all cases, nonlinear models have lower AIC than linear models. This comparison verifies the use of quadratic temperature (T^2) and precipitation (P^2) terms.

To synthesize joint multifactor global change effects, we used the fitted models to predict primary production in the four-dimensional environment space (T, P, C, and N) without fires, spanning the entire experiment. We set up continuous gradients for temperature (8.69–12.28 °C) and precipitation (240–1,380 mm), as well as categorical levels for CO_2 (ambient 409 $\mu mol \cdot mol^{-1}$, elevated 680 $\mu mol \cdot mol^{-1}$) and nitrogen (ambient 0.25 $g \cdot m^{-2} \cdot y^{-1}$, elevated 7.25 $g \cdot m^{-2} \cdot y^{-1}$). We visualized our predictions by temperature and precipitation interaction at different CO_2 and nitrogen level combinations. We summarized the modeled NPP, overlaid with observed NPP in Fig. 3. We included similar surfaces for ANPP and BNPP in Figs. S3 and S4.

To assess model performance, we compared modeled vs. observed primary production, summarized by goodness-of-fit measures. The modeled values were calculated as the expected (or fitted) primary production given environmental variables at unique temperature–precipitation–CO_2–nitrogen combinations. These modeled values were then compared with the observed primary production. Fig. S5*A* shows that the modeled and observed NPP, ANPP, and BNPP are close to the 1:1 reference line. We then summarized their goodness of fit by Pearson correlation coefficient, which is a measure between −1 and +1, where a higher value indicates a better fit. For all groups, the modeled and observed primary production are highly correlated (r_{NPP} = 0.64, r_{ANPP} = 0.68, and r_{BNPP} = 0.54). This assessment validates that the model can predict the data well.

To check model assumptions, we performed residual diagnostics, focusing on progressive (year-dependent) effects. Progressive year effects would result in model residuals (unexplained component of observed data) that correlate with year. Residual diagnostics in Fig. S5*B* show that the residuals are not correlated with year, providing additional evidence of the absence of progressive effects. Fig. S5*C* validates the normality assumption of the model residuals, supporting log-transformed NPP variables.

All analyses were performed in R version 3.2.4 (34). All data and code are available upon request.

ACKNOWLEDGMENTS. We thank Jeffrey Dukes, Bruce Hungate, Yiqi Luo, and Erika Zavaleta for comments on the manuscript. The study was supported by the National Science Foundation, US Department of Energy, Packard Foundation, Morgan Family Foundation, Alexander von Humboldt Foundation, Stanford University, and Carnegie Institution for Science.

1. Dieleman WI, et al. (2012) Simple additive effects are rare: A quantitative review of plant biomass and soil process responses to combined manipulations of CO_2 and temperature. *Glob Change Biol* 18(9):2681–2693.
2. Leuzinger S, et al. (2011) Do global change experiments overestimate impacts on terrestrial ecosystems? *Trends Ecol Evol* 26(5):236–241.
3. Langley JA, Hungate BA (2014) Plant community feedbacks and long-term ecosystem responses to multi-factored global change. *AoB Plants* 6:6.
4. Niboyet A, et al. (2011) Testing interactive effects of global environmental changes on soil nitrogen cycling. *Ecosphere* 2(5):1–24.
5. Zavaleta ES, et al. (2003) Plants reverse warming effect on ecosystem water balance. *Proc Natl Acad Sci USA* 100(17):9892–9893.
6. Cleland EE, Chiariello NR, Loarie SR, Mooney HA, Field CB (2006) Diverse responses of phenology to global changes in a grassland ecosystem. *Proc Natl Acad Sci USA* 103(37):13740–13744.
7. Zavaleta ES, et al. (2003) Grassland responses to three years of elevated temperature, CO_2, precipitation, and N deposition. *Ecol Monogr* 73(4):585–604.
8. Gutknecht JLM, Field CB, Balser TC (2012) Microbial communities and their responses to simulated global change fluctuate greatly over multiple years. *Glob Change Biol* 18(7):2256–2269.
9. Peters HA, et al. (2007) Responses of temporal distribution of gastropods to individual and combined effects of elevated CO_2 and N deposition in annual grassland. *Acta Oecol* 31(3):343–352.
10. LeBauer DS, Treseder KK (2008) Nitrogen limitation of net primary productivity in terrestrial ecosystems is globally distributed. *Ecology* 89(2):371–379.
11. Lee M, Manning P, Rist J, Power SA, Marsh C (2010) A global comparison of grassland biomass responses to CO_2 and nitrogen enrichment. *Philos Trans R Soc Lond B Biol Sci* 365(1549):2047–2056.
12. Sillen WMA, Dieleman WIJ (2012) Effects of elevated CO_2 and N fertilization on plant and soil carbon pools of managed grasslands: A meta-analysis. *Biogeosciences* 9(6): 2247–2258.
13. Shaw MR, et al. (2002) Grassland responses to global environmental changes suppressed by elevated CO_2. *Science* 298(5600):1987–1990.
14. Dukes JS, et al. (2005) Responses of grassland production to single and multiple global environmental changes. *PLoS Biol* 3(10):e319.
15. Norby RJ, et al. (2007) Ecosystem responses to warming and interacting global change factors. *Terrestrial Ecosystems in a Changing World*. Global Change – The IGBP Series, eds Canadell JG, Pataki DE, Pitelka LF (Springer, Berlin), pp 23–36.
16. Lunch CK (2009) Primary productivity in an annual grassland ecosystem: Responses to global change and local environmental variation. PhD dissertation (Stanford University, Stanford, CA).
17. Nowak RS, Ellsworth DS, Smith SD (2004) Functional responses of plants to elevated atmospheric CO_2—Do photosynthetic and productivity data from FACE experiments support early predictions? *New Phytol* 162(2):253–280.
18. Morgan JA, et al. (2011) C4 grasses prosper as carbon dioxide eliminates desiccation in warmed semi-arid grassland. *Nature* 476(7359):202–205.
19. Sharkey TD (1985) Photosynthesis in intact leaves of C3 plants: Physics, physiology and rate limitations. *Bot Rev* 51(1):53–105.
20. Duncan DA, Woodmansee RG (1975) Forecasting forage yield from precipitation in California's annual rangeland. *J Range Manage* 28(4):327–329.
21. Murphy AH (1970) Predicted forage yield based on fall precipitation in California annual grasslands. *J Range Manage* 23(5):363–365.
22. Suttle KB, Thomsen MA, Power ME (2007) Species interactions reverse grassland responses to changing climate. *Science* 315(5812):640–642.
23. Yang YH, Fang JY, Ma WH, Wang W (2008) Relationship between variability in aboveground net primary production and precipitation in global grasslands. *Geophys Res Lett* 35(23), 10.1029/2008GL035408.
24. Hsu JS, Powell J, Adler PB (2012) Sensitivity of mean annual primary production to precipitation. *Glob Change Biol* 18(7):2246–2255.
25. Ruppert JC, et al. (2012) Meta-analysis of ANPP and rain-use efficiency confirms indicative value for degradation and supports non-linear response along precipitation gradients in drylands. *J Veg Sci* 23(6):1035–1050.
26. Luo Y, et al. (2004) Progressive nitrogen limitation of ecosystem responses to rising atmospheric carbon dioxide. *Bioscience* 54(8):731–739.
27. Oechel WC, et al. (2000) Acclimation of ecosystem CO_2 exchange in the Alaskan Arctic in response to decadal climate warming. *Nature* 406(6799):978–981.
28. NOAA Earth Systems Research Laboratory (2016) Trends in atmospheric carbon dioxide (National Oceanic And Atmospheric Administration, Boulder, CO).
29. Higgins PAT, Jackson RB, Des Rosiers JM, Field CB (2002) Root production and demography in a california annual grassland under elevated atmospheric carbon dioxide. *Glob Change Biol* 8(9):841–850.
30. Farquhar GD, Ehleringer JR, Hubick KT (1989) Carbon isotope discrimination and photosynthesis. *Annu Rev Plant Physiol* 40:503–537.
31. Ainsworth EA, Long SP (2005) What have we learned from 15 years of free-air CO_2 enrichment (FACE)? A meta-analytic review of the responses of photosynthesis, canopy properties and plant production to rising CO_2. *New Phytol* 165(2):351–371.
32. NADP (2014) Total deposition maps (National Atmospheric Deposition Program, Champaign, IL).
33. Bolker BM, et al. (2009) Generalized linear mixed models: A practical guide for ecology and evolution. *Trends Ecol Evol* 24(3):127–135.
34. R Development Core Team (2016) *R: A Language and Environment for Statistical Computing* (R Foundation for Statistical Computing, Vienna).

Supporting Information

Zhu et al. 10.1073/pnas.1606734113

SI Text

Here we show the mathematical details of the analyses.

Exploratory Analysis. For plot i, year t, the response variable NPP (or ANPP, BNPP) is y_{it}. To test for year-dependent treatment effects, we first performed standard ANOVAs separately for each year,

$$\log(y_{it}) = Z_{it}\gamma_t + \delta_{it}, \quad \text{[S1]}$$

where Z_{it} is the design matrix with main and interaction terms (0: plot with ambient treatment; 1: plot with elevated treatment), γ_t's are treatment effects (ANOVA coefficients) across years (t), and δ_{it} is random error. Across all of the single-factor and interactive effects, there are no consistent temporal trends in the treatment effects (γ_t) that are significant at $P < 0.05$ (Fig. S2).

To integrate the experimental treatments and natural variation, we plotted the response variable NPP (or ANPP, BNPP) y_{it}, against actual temperature T_{it}, precipitation P_{it}, CO_2 C_{it}, and nitrogen N_{it}. Fig. 1 shows the pairwise relationships between the responses (averaged on log scale, mean ± SE) and each of the predictors: y_{it} vs. T_{it}, y_{it} vs. P_{it}, y_{it} vs. C_{it}, and y_{it} vs. N_{it}. Note that these are marginal relationships that do not account for interactions among predictors. We fitted theses marginal relationships with linear and quadratic functions, which motivates our functional choice in the joint modeling.

Joint Modeling. We developed the following linear mixed-effects model to jointly quantify how NPP and its components respond to global changes across experimental manipulation and natural variation:

$$\log(y_{it}) = X_{it}\beta + b_i + \varepsilon_{it}, \quad \text{[S2]}$$

where the response $\log(y_{it})$ is log-transformed NPP (or ANPP, BNPP), a design matrix X_{it} includes global changes across treatment and year, a fixed effect β quantifies main and interactive environmental effects, a random effect b_i quantifies the plot-specific effect on NPP, and random error ε_{it} is assumed to be independent and normally distributed with mean 0 and variance σ^2,

$$\varepsilon_{it} \sim N(0, \sigma^2). \quad \text{[S3]}$$

The design matrix is

$$\begin{aligned} X_{it} = [&T^2, P^2, T, P, C, N \\ &TP, TC, TN, PC, PN, CN, \\ &TPC, TPN, TCN, PCN, \\ &TPCN, \\ &F03, B11]_{it}, \end{aligned} \quad \text{[S4]}$$

where T is standardized temperature, P is standardized precipitation, C is standardized CO_2, N is standardized nitrogen, $F03$ is a factor variable denoting whether or not the plot was burned in the 2003 wildfire, and $B11$ is a factor variable denoting whether or not the plot was burned in the 2011 control burn. Correspondingly, the estimated environmental effects are

$$\begin{aligned} \beta = [&\underbrace{\beta_{T^2}, \beta_{P^2}, \beta_T, \beta_P, \beta_C, \beta_N,}_{\text{main effect}} \\ &\underbrace{\beta_{TP}, \beta_{TC}, \beta_{TN}, \beta_{PC}, \beta_{PN}, \beta_{CN},}_{\text{two-way interaction}} \\ &\underbrace{\beta_{TPC}, \beta_{TPN}, \beta_{TCN}, \beta_{PCN},}_{\text{three-way interaction}} \\ &\underbrace{\beta_{TPCN},}_{\text{four-way interaction}} \\ &\underbrace{\beta_{F03}, \beta_{B11}]}_{\text{fire effect}}. \end{aligned} \quad \text{[S5]}$$

Because we focus on environmental effects in this analysis, we presented only T, P, C, and N coefficients in the main text but included $F03$ and $B11$ coefficients in Table S1. The estimated β's are plotted in Fig. 2 (except fire effects are presented in Table S1).

The nonlinear (quadratic) terms T^2 and P^2 are justified by comparing a quadratic model with design matrix **S4** vs. a linear model with the following design matrix:

$$\begin{aligned} X_{it} = [&T, P, C, N, \\ &TP,\ TC,\ TN,\ PC,\ PN,\ CN, \\ &TPC,\ TPN,\ TCN,\ PCN, \\ &TPCN, \\ &F03, B11]_{it}. \end{aligned} \quad \text{[S6]}$$

We then calculated the AICs for both models and found that nonlinear models always have lower AICs (Table S2).

Response Surface Analysis. The multidimensional surfaces were model predictions based on setting all possible combinations of T, P, C, and N and setting $F03$ and $B11$ to ambient levels:

$$\log(\tilde{y}) = \tilde{X}\hat{\beta}, \quad \text{[S7]}$$

where $\tilde{y}$ is predicted NPP (or ANPP, BNPP), $\tilde{X}$ includes standardized T and P gradients, C and N levels, and ambient $F03$ and $B11$, $\hat{\beta}$ is estimated environmental effects in Fig. 2 and Table S1. Fig. 3 and Figs. S3 and S4 present the predicted $\tilde{y}$ (surfaces and contour lines) as well as the observed y_{it} (bubbles).

Model Assessment. We performed in-sample prediction to assess model performance,

$$\log(\tilde{y}_{it}) = X_{it}\hat{\beta} + \hat{b}_i, \quad \text{[S8]}$$

where $\hat{y}_{it}$ is fitted (modeled) NPP (or ANPP, BNPP), X_{it} is the observed environment, $\hat{\beta}$ is estimated fixed effect, and $\hat{b}_i$ is estimated random effect. We first compared modeled ($\hat{y}_{it}$) vs. observed (y_{it}) NPP and its components in Fig. S5*A*. We also calculated the correlation between $\hat{y}_{it}$ and y_{it}.

We then performed residual diagnostics to check whether the model assumption **S3** has been satisfied. The estimated residual is

$$\hat{\varepsilon}_{it} = \log(y_{it}) - \log(\hat{y}_{it}). \quad \text{[S9]}$$

The plot of residuals against year in Fig. S5*B* shows independence of year (no progressive year effect). The histogram of residuals in Fig. S5*C* shows normality.

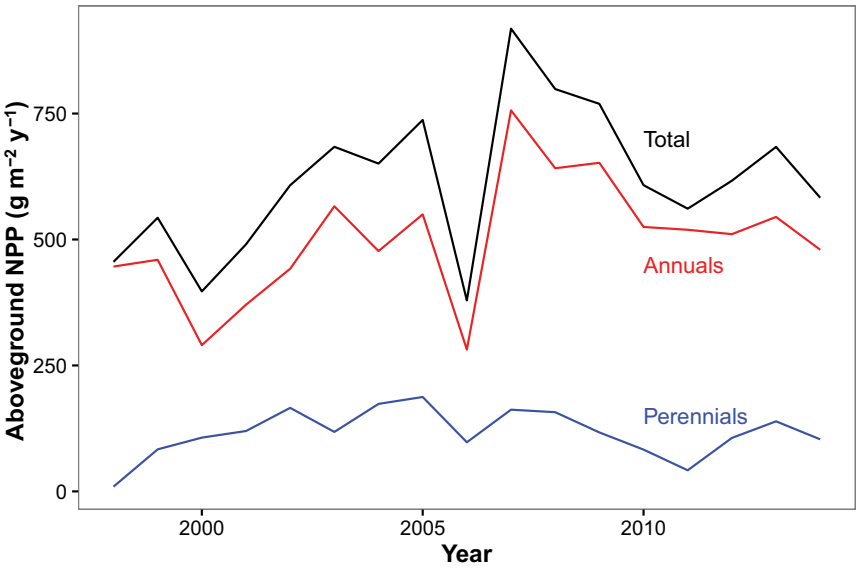

Fig. S1. Total ANPP (black line) and the component from annual plants (red line) and perennials (blue line) averaged across all treatments, from 1998 through 2014.

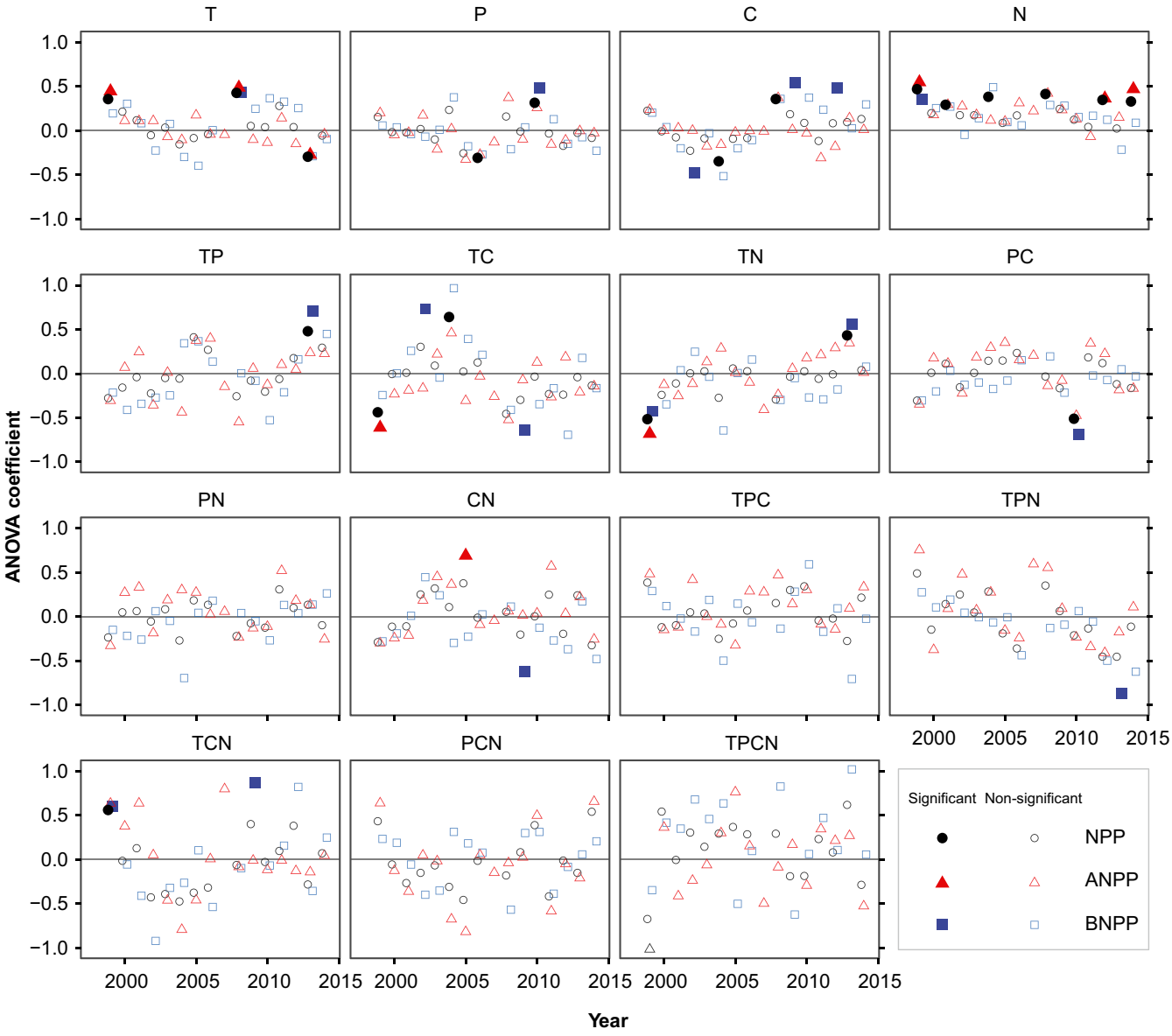

Fig. S2. ANOVA coefficients across years to test treatment effects over years. Filled symbols are significant at $P < 0.05$; unfilled symbols are nonsignificant.

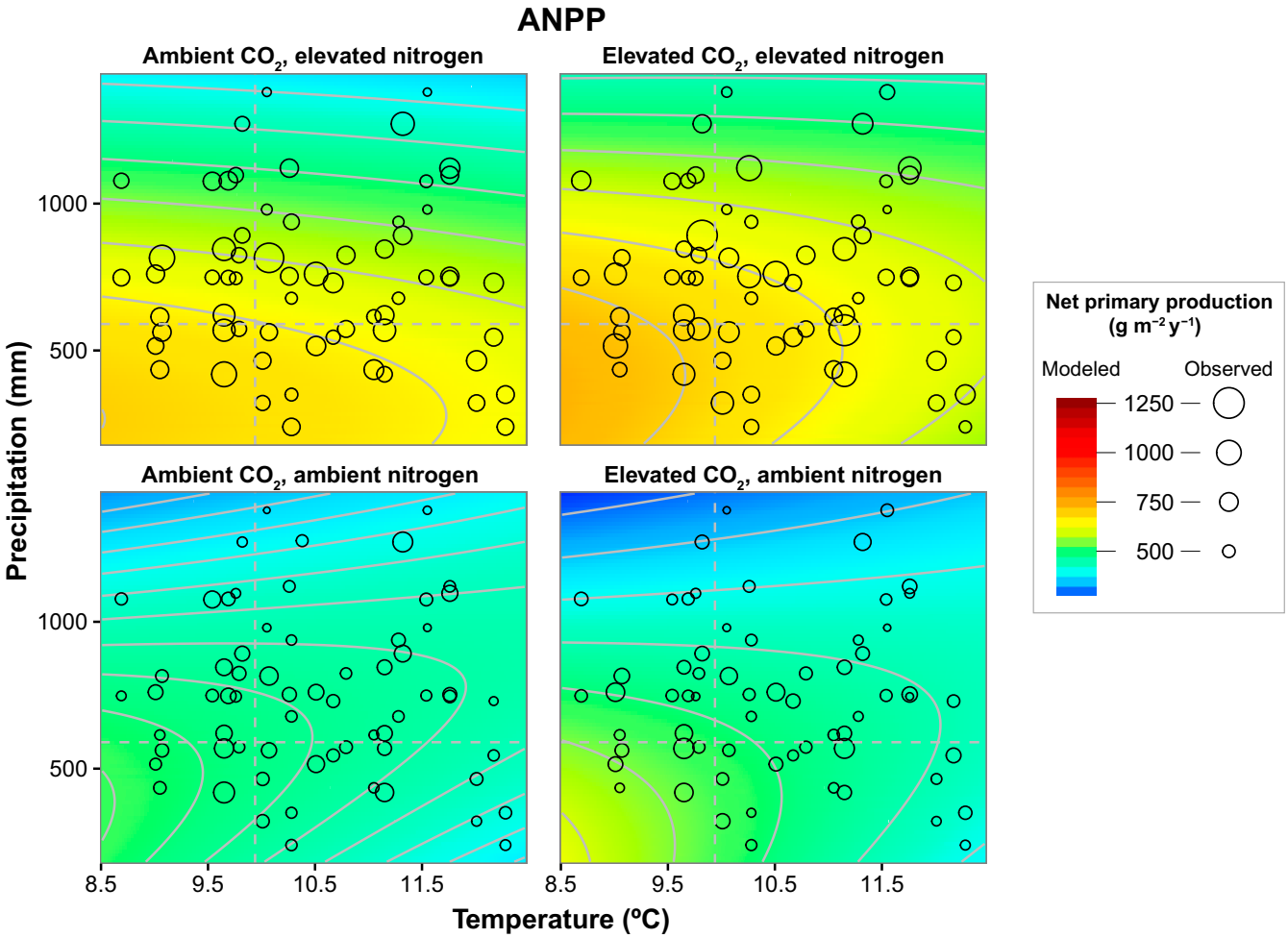

Fig. S3. Modeled and observed ANPP in four-dimensional temperature–precipitation–CO_2–nitrogen space. Symbols follow Fig. 3.

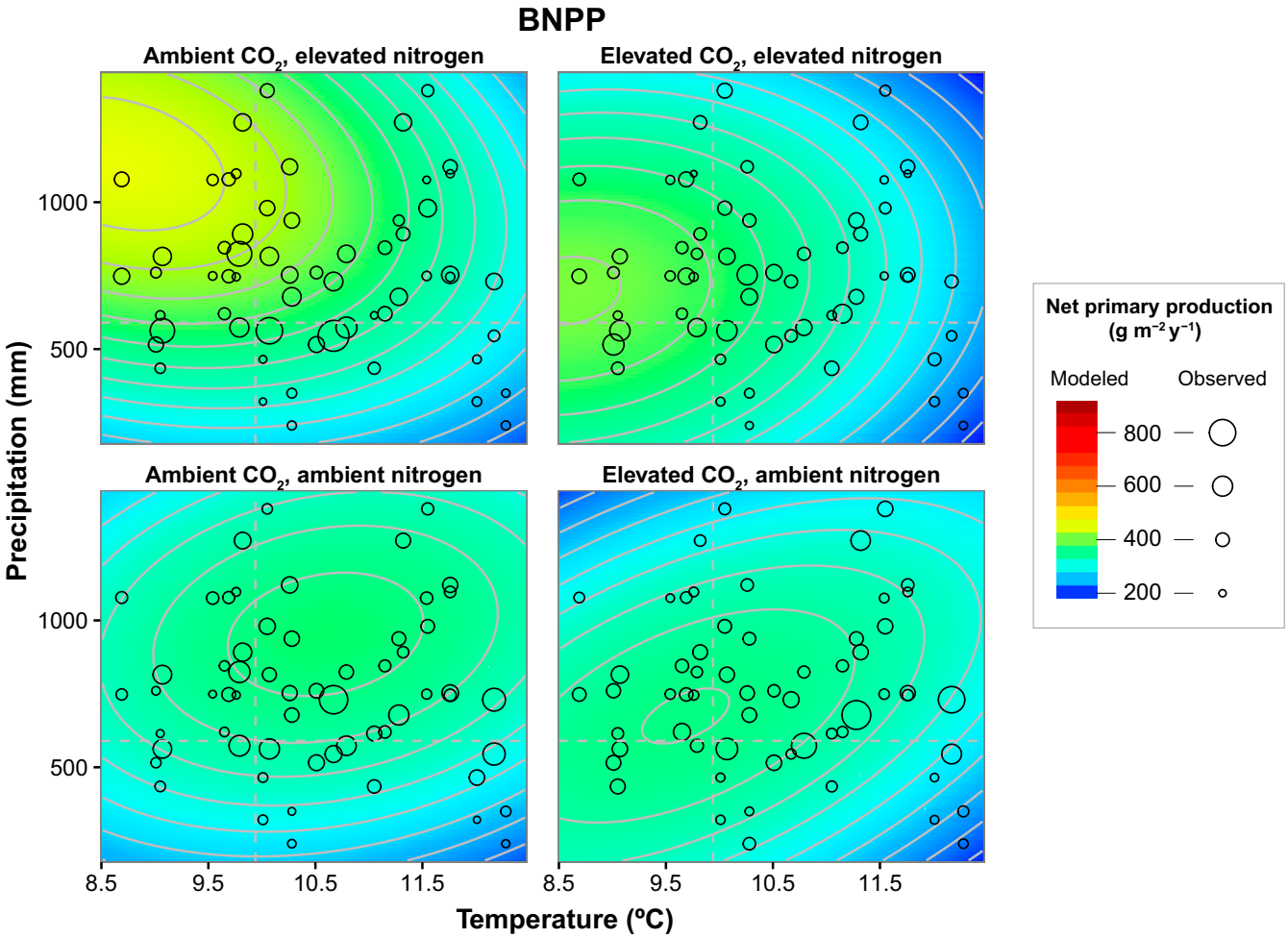

Fig. S4. Modeled and observed BNPP in four-dimensional temperature–precipitation–CO_2–nitrogen space. Symbols follow Fig. 3.

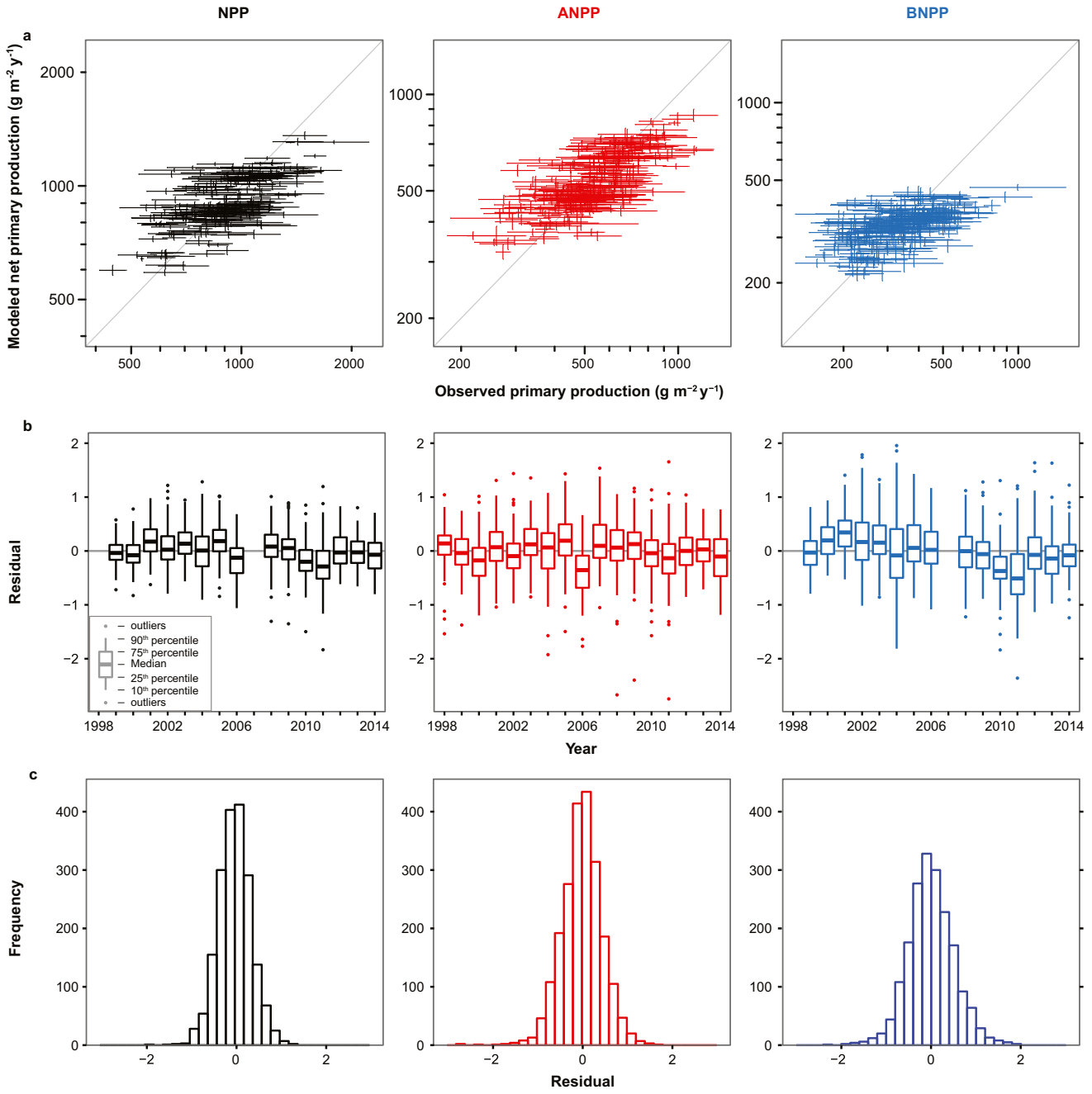

Fig. S5. Model assessment. (*A*) modeled vs. observed NPP, where each crosshair is NPP (mean ± SE) in a unique temperature–precipitation–CO_2–nitrogen–fire combination. (*B*) Residuals over years to test for progressive effects. (*C*) Residual distribution to test for normality assumption.

Table S1. Model coefficients (mean and 95% confidence intervals)

Coefficient	NPP	ANPP	BNPP
T^2	−0.008 (–0.023, 0.008)	−0.002 (–0.021, 0.017)	−0.033 (–0.054, –0.011)
P^2	−0.053 (–0.069, –0.037)	−0.036 (–0.055, –0.017)	−0.054 (–0.076, –0.031)
T	−0.027 (–0.046, –0.005)	−0.028 (–0.054, –0.002)	−0.065 (–0.095, –0.033)
P	−0.016 (–0.036, 0.004)	−0.080 (–0.103, –0.056)	0.042 (0.013, 0.071)
C	−0.000 (–0.021, 0.020)	0.017 (–0.011, 0.044)	−0.028 (–0.063, 0.007)
N	0.101 (0.081, 0.122)	0.141 (0.113, 0.169)	0.021 (–0.015, 0.057)
TP	0.020 (0.002, 0.038)	0.022 (–0.001, 0.044)	0.013 (–0.013, 0.039)
TC	−0.013 (–0.031, 0.005)	−0.007 (–0.031, 0.016)	−0.019 (–0.046, 0.008)
TN	−0.021 (–0.039, –0.003)	−0.001 (–0.024, 0.022)	−0.044 (–0.071, –0.017)
PC	−0.003 (–0.024, 0.018)	−0.003 (–0.026, 0.021)	−0.045 (–0.075, –0.014)
PN	−0.008 (–0.027, 0.010)	−0.016 (–0.038, 0.006)	0.005 (–0.022, 0.032)
CN	−0.002 (–0.022, 0.018)	0.018 (–0.009, 0.044)	−0.021 (–0.055, 0.014)
TPC	0.009 (–0.009, 0.028)	0.007 (–0.017, 0.030)	0.017 (–0.010, 0.044)
TPN	−0.016 (–0.033, 0.001)	−0.014 (–0.035, 0.007)	−0.018 (–0.042, 0.006)
TCN	0.002 (–0.015, 0.020)	0.000 (–0.022, 0.023)	0.001 (–0.025, 0.028)
PCN	0.005 (–0.016, 0.026)	0.028 (0.004, 0.052)	−0.009 (–0.039, 0.021)
TPCN	0.003 (–0.015, 0.022)	0.000 (–0.023, 0.024)	0.001 (–0.025, 0.028)
F03	0.154 (0.005, 0.302)	0.299 (0.112, 0.485)	0.047 (–0.163, 0.256)
B11	0.274 (0.147, 0.401)	0.361 (0.201, 0.519)	0.138 (–0.040, 0.317)

Notations follow Fig. 2.

Table S2. Comparison of the linear vs. nonlinear model based on AIC for NPP, ANPP, and BNPP data

Model	NPP	ANPP	BNPP
Linear model	1,857	3,718	3,254
Nonlinear model	1,817	3,168	3,226

Nonlinear models are preferred due to lower AIC.